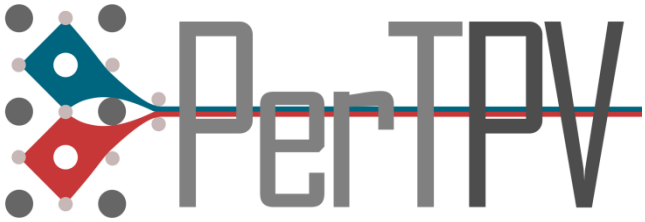

PerTPV – Perovskite thin film photovoltaics

Grant agreement 763977

Deliverable number 5.2 (PUBLIC, demonstrator)

Deliverable Title: Deliver a 15% efficient flexible single junction mini-module

WP5

Lead beneficiary: VTT
Authors: Riikka Suhonen, Ville Holappa, VTT and Adriana Paracchino, CSEM, Daniel Pérez-del-Rey, Arghanoon Moeini, Abhyuday Paliwal, Henk J. Bolink, UVEG and Henry Snaith, UOXF
Delivery date: 31/07/2021
Confidentiality level: Public

The PerTPV project has received funding from the European Union's Horizon 2020 research and innovation programme under grant agreement No 763977.

Revision History

Author Name, Partner short name	Description	Date
Riikka Suhonen, Ville Holappa, VTT and Adriana Paracchino, CSEM	Draft deliverable	8/7/2021
Daniel Pérez-del-Rey, Arghanoon Moeini, Abhyuday Paliwal and Henk J. Bolink, UVEG	Revision 1	28/7/2021
Henry Snaith, UOXF	Final	17/8/2021

Contents

The PerTPV project has received funding from the European Union's Horizon 2020 research and innovation programme under grant agreement No 763977.

Description and objectives

This deliverable is related to the following objectives of PerTPV:

- **O2.4:** *Develop manufacturing compatible solvent/ink formulations for perovskite absorber layers and complete material set in the solar cell stack*.
- **O5.3:** *Deliver a production line materials-set, tool-set and manufacturing specification ready for cost analysis and specification of pilot-scale manufacturing*.

For printable perovskite solar cells to be a viable reality, industrially acceptable solvents must be employed. Thus, a lot of effort was put on PerTPV **Task 2.1**: *Benign solvent and ink development*. The ultimate goal of PerTPV was to use the developed inks from benign solvents in the flexible single junction minimodules to simultaneously accomplish both **O2.4** and **O5.3**.

The first results from **Task 2.1** have been reported in **D2.3:** *Report on ink preparation using benign solvents*. But due to the importance of this task, the development efforts were extended beyond the results from **D2.3** and are reported in Section 1. The results from developments of flexible mini-modules are reported in Section 2.

1. Perovskite inks from benign solvents

Here, approaches to develop inks for both 1-step and 2-step conversion from precursors to perovskite were followed.

For the 1-step conversion, Cyrene (dihydrolevoglucosenone) based inks developed at UOXF were studied whereas for 2-step conversion, lead iodide (PbI_2) particle inks in mixed alcohols were developed at VTT. The results are described in the following Sections 1.1 and 1.2.

1.1 Cyrene:water inks for 1-step conversion

1.1.1 Cyrene:water ink developments

Cyrene as a solvent simplifies the processing conditions of the perovskite film because no antisolvent is required.

In **D2.3:** *Report on ink preparation using benign solvents*, the studied ink composition was formamidinium-cesium lead iodide-bromide perovskite (0.53M Pb) dissolved in Cyrene:DMSO 3:1 (v:v).

In the newly formatted recipe ($PbAc_2$:PbI_2:MACl:FAI = 1 : 1 : 2 : 4), the $FAPbI_3$-perovskite was formed via a dual-source Pb-precursor approach and the solvent system was Cyrene:water (H_2O) in 85:15 (v:v). Cyrene forms a geminal diol with H_2O and in combination with the lead acetate ($PbAc_2$), results in high viscous, honey-like ink.

At UOXF, homogenous layers were achieved on top of rigid and porous FTO/SnO_2/Al_2O_3 substrates by using heated substrates, warm ink and high temperature (200°C) annealing. At VTT for flexible substrates, the processing needed to be modified because the maximum annealing temperature for flexible PET substrate is 140°C.

Altogether, about 20 different ink compositions including the diluted inks were tested at VTT during the project. The tested variables are listed below:

- **Additives:** CsBr, CsI and MAI
- **Substrates:** PET/ITO/SnO_2, PET/ITO/PEDOT:PSS and PET/ITO/SnO_2+Al_2O_3
- **Annealing conditions:** gas-quenching pre-anneal with nitrogen (N2) or hot-air blow, annealing in IR-ovens or normal oven, anti-solvent bath, printing on warm substrate with warm ink

Concentrations and viscosity curve of two inks are shown in Figure 1. Both inks show a slightly shear thinning behaviour which is desirable for printing. The initial viscosity of Ink 8 is in the optimal range (0.05-0.5 Pa·s) for gravure printing, whereas Ink 1 has a slightly

The PerTPV project has received funding from the European Union's Horizon 2020 research and innovation programme under grant agreement No 763977.

too low viscosity. As seen in the photograph in Figure 1c), the resolution of the printed patterns is good but the perovskite conversion is not complete (no appearance of the dark colour characteristic to perovskite).

a)

Cyrene-H2O inks		**INK 1:** Decrease the overall concentration (50% of the original ink) PbAc2 : PbI2 : MACl : FAI = 1 : 1 : 2 : 4	**INK 8:** Decrease the overall concentration (75% of the original ink) and add CsI PbAc2 : PbI2 : MACl : FAI : CsI = 1 : 1 : 2 : 3.8 : 0.2
PbAc2	g	0.1517	0.2276
PbI2	g	0.1844	0.2766
MACl	g	0.0540	0.0810
FAI	g	0.2752	0.3921
CsI	g		0.0312
Cyrene:H2O	ml	3	3

b)

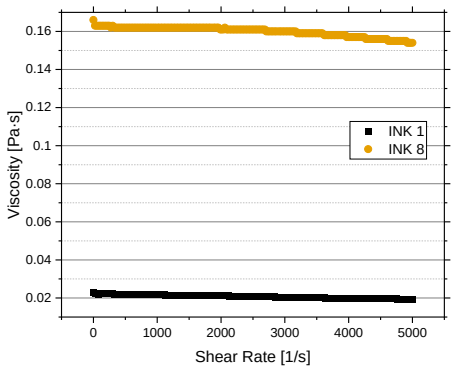

c)

Figure 1. a) Ink recipes and b) the corresponding viscosity curves as a function of increasing shear rate. In c) a digital photograph of the printed layer (Ink 8) taken on top of a white light illuminating table is shown. Substrate was PET/ITO/SnO_2.

Due to the challenges in the perovskite conversion, a recipe from literature[1] was also tested to confirm the possibility for conversion. In Figure 2a), a photograph of a printed layer from ink dissolved solely in DMF is shown. Based only on the visual observation, the conversion to perovskite appears to happen with the DMF-ink. According to Zwang et.al.[2]; "*During the solution coating process, solvent evaporation occurs but the excess organic component remains within the film, the removal of which by following thermal annealing leads to the fully crystallized perovskite thin film*". Thus, the following processes should take place:

- PbI_2·DMF + FAI = $FAPbI_3$ + DMF (g)
- $PbAc_2$ + 3MAI = $MAPbI_3$ + 2MA·Ac (g)

And additionally, with annealing temperature ≥120°C, a stable α-phase mixed-cation (MA/FA) perovskite should be formed.

[1] D. Luo et.al., Adv. Mater., 2017, 29, 1604758, Dual-Source Precursor Approach for Highly Efficient Inverted Planar Heterojunction Perovskite Solar Cells
https://onlinelibrary.wiley.com/doi/full/10.1002/adma.201604758

[2] W. Zhang et.al., Nat. Commun., 2015, 6:6142, doi: 10.1038/ncomms7142, Ultrasmooth organic–inorganic perovskite thin-film formation and crystallization for efficient planar heterojunction solar cells.
https://www.nature.com/articles/ncomms7142/

The PerTPV project has received funding from the European Union's Horizon 2020 research and innovation programme under grant agreement No 763977.

Due to the limited solubility of MAI in Cyrene: H_2O mixed solvent, the literature recipe as such resulted in a hazy, undissolved ink. Nevertheless, a few printing trials were made with the ink and one of the printed layers is shown in Figure 2b). It is worth to mention that a gas-quenching step prior to thermal annealing was found to improve the perovskite layer quality. With the ink in DMF, the gas-quenching time (N_2-gas blowing until the edges of the printed pattern turned brown) was only 14 seconds whereas for the inks in Cyrene: H_2O, the gas-quenching time was significantly increased to 5 minutes. Though a brown colour characteristic to perovskite appeared partly in the printed layers, the solubility issues resulted into an unstable ink and requiring modification of the recipe.
MACl was exploited as an additive increasing the solubility of other pre-cursors in Cyrene:H_2O. Even with MACl, the ink had to be diluted to 75% of the original concentration in DMF to dissolve all the pre-cursors. Still, as shown in Figure 2c), high quality print layers were achieved with the "precursor phase" but no perovskite formation appeared with the ink, identified by the fact that the layers remained yellowish in colour.

a) Fully dissolved, $PbAc_2$:PbI_2:MAI:FAI = 0.6 : 0.4 : 1.8 : 0.4 in DMF (literature recipe 1M Pb^{2+} from dual source) N_2-blow / 14s + oven 140°C/30min	**b) Partially dissolved,** $PbAc_2$:PbI_2:MAI:FAI = 0.6 : 0.4 : 1.8 : 0.4 : 1 in Cyrene:H_2O (85:15 v:v ratio, diluted 1:1 with EtOH) N_2-blow / 5min + oven 140°C/30min	**c) Fully dissolved,** $PbAc_2$:PbI_2:MAI:FAI:MACl = 0.6 : 0.4 : 1.8 : 0.4 : 1 in Cyrene:H_2O (85:15 v:v ratio, 75% of the original concentration in DMF) N_2-blow / 5min + oven 140°C/30min
		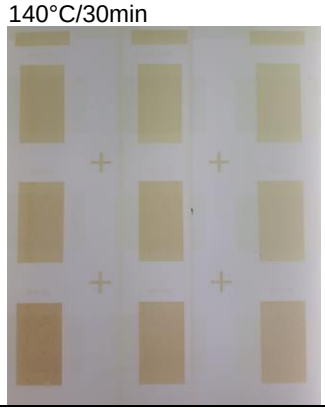

Figure 2. Recipes of inks and digital photographs of the printed layers taken on top of a white light illuminating table. Substrate in all samples was PET/ITO/SnO_2.

1.1.2 Summary and conclusions

To summarize, the Cyrene:H_2O solvent system results into very good printing inks with desired rheological properties. But due to the challenges in the conversion of the printed layer to perovskite, specifically due to the requirement to remain at or below 140C, and due to the diminishing resources towards the end of the project, the developments could not be pursued further within this project.

1.2 PbI_2 inks for 2-step conversion

The objective in this work was to print a porous lead iodide (PbI_2) layer from nanocrystals dispersed in a benign solvent. The porous PbI_2 would later be converted into perovskite in the following process step.

1.2.1 PbI_2 dispersion

In order to achieve a uniform PbI_2 layer, the first task was to make a stable dispersion from the PbI_2 powder. Typically, there are three approaches that can be followed when making a dispersion:

1) Charging the particles,
2) Separation of particles by a ligand, or

The PerTPV project has received funding from the European Union's Horizon 2020 research and innovation programme under grant agreement No 763977.

3) Increase the viscosity of the solution supporting the particles.

At first, the approach of utilizing citric acid (and later also other materials) as a ligand separating the PbI_2-particles from agglomerating was followed. The PbI_2 pellets were ground to a fine powder with a ball mill and then dispersed in citric acid (CA) solution in ethanol by ultrasonication. Citric acid was chosen as the ligand that interacts with the PbI_2 particles and prevents aggregation by keeping the particles separated from each other. Several PbI_2 and citric acid concentrations were tested to improve stability of the ink (and the quality of the printed PbI2 layers) and these are listed in Table 1.

Table 1. The tested lead iodide and citric acid concentrations.

#	PbI_2 [g/ml]	Citric acid [g/ml]	Solvent system
1	2.0	0.35	Ethanol
2	2.0	0.5	Ethanol
3	1.0	0.6	Ethanol
4	2.0	0.35	Ethanol:Buthanol 7:3
5	2.0	0.6	Ethanol:2-butoxyethanol 7:3
6	2.0	0.35	Ethanol:2-butoxyethanol 7:3

All of the inks listed in Table 1, were fabricated via Method 1 which is depicted in Figure 3a). It proved to be challenging to prepare a stable dispersion this way. However, the ink was used to print PbI_2 films by gravure printing. As shown in Figure 3a), the unstable dispersion resulted in discontinuous layer as the ink did not spread evenly on top of the PET/ITO/SnO_2 -substrate.

Method 1 was then modified to Method 2 where the PbI_2 powder and citric acid crystals were ground together to make sure the materials have stronger interactions. This powder was then mixed with ethanol and/or the mixture of ethanol and 2-butoxyethanol with a ratio of 3:7 (v:v). The mixing was done with an ultrasonic finger. By grinding both solid materials together before dispersing them in the solvent resulted in a more stable ink and improved the print quality (Figure 3b)). Even though the PET/ITO/SnO_2 substrate was still not fully covered, the particle size was decreased indicating that grinding is a more efficient way to contact the PbI_2 and citric acid powders.

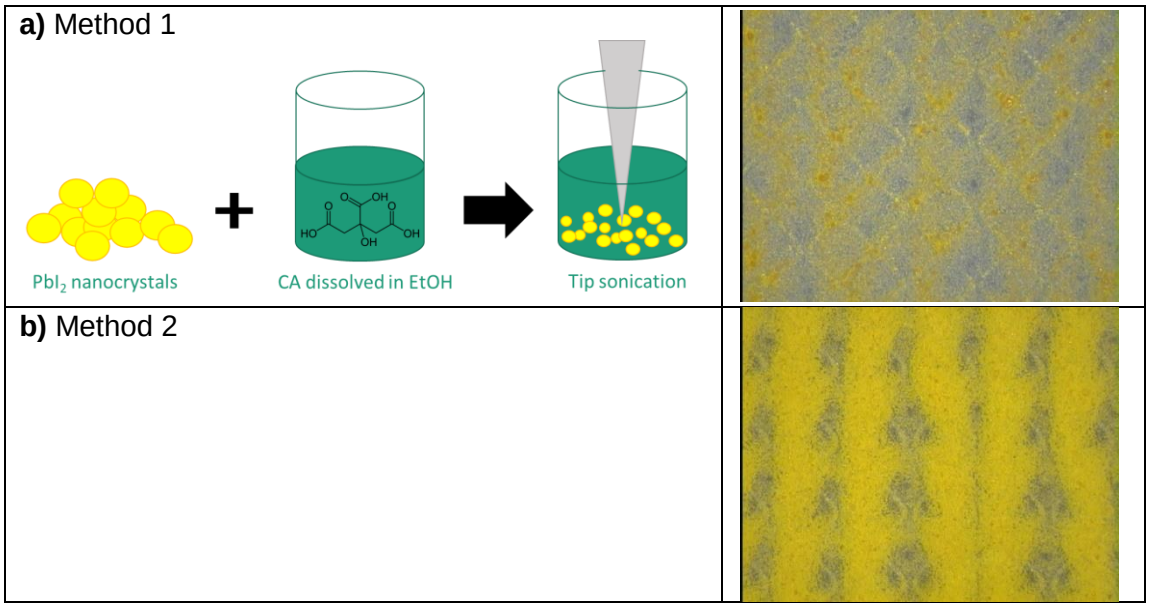

The PerTPV project has received funding from the European Union's Horizon 2020 research and innovation programme under grant agreement No 763977.

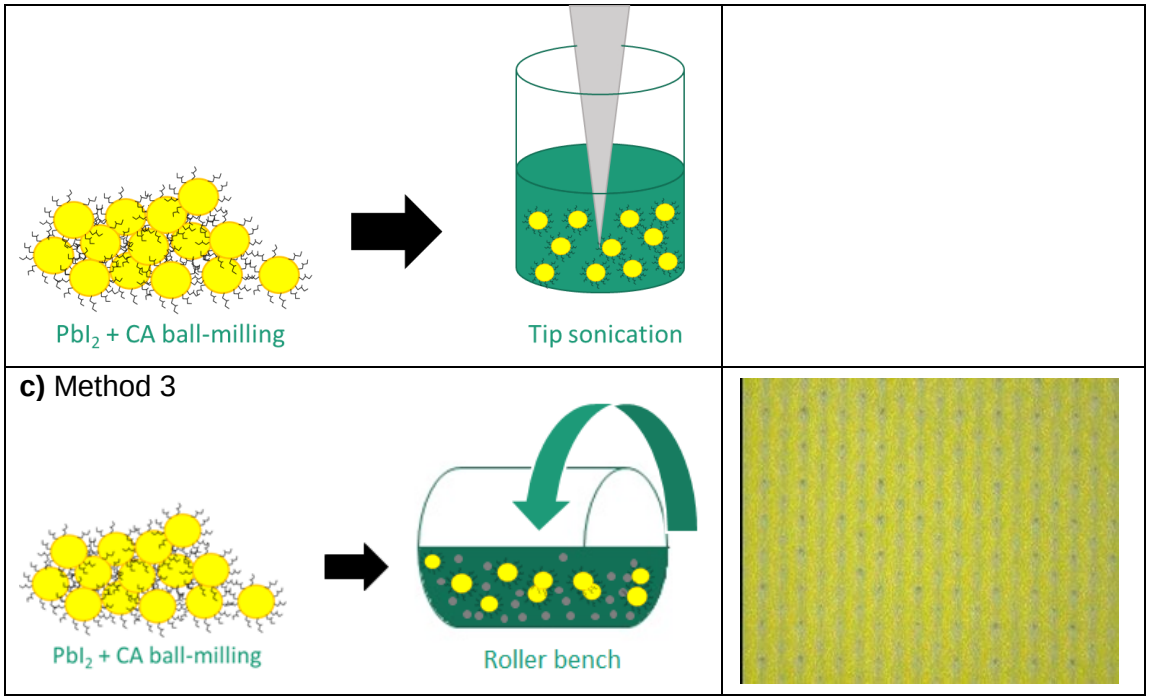

Figure 3. (Left) Depiction of the methods utilized in the fabrication of the PbI_2 dispersion. (Right) Optical microscopic images (magnification 202x) of the corresponding printed PbI_2 layers where the printing inks are made following the methods described on the left.

In addition to citric acid and ethanol:2-butoxyethanol, several ligands and solvents were also tested.

- **Ligands:** butylamine, octylamine, oleylamine, acetohydroxamic acid, benzhydroxamic acid, polyacrylic acid (PAA) and poly(4-vinyl pyrrolidone) (PVP)
- **Solvents:** EDGA, PGMEA, 2-butoxyethyl acetate and water

But none of the listed combinations resulted into a stable dispersion prepared with the Method 2.

As it became obvious that ultrasonication was an insufficient way to achieve a stable dispersion, another mixing method was tested. In Method 3 (shown in Figure 3c)), the ink vial was placed on a roller bench where it was rotated for one week at room temperature. This method introduced continuous grinding by the mixing balls (ZrO, d = 0.5 cm) that eventually led to smaller PbI_2 particles and smoother printed films. Still, the dispersion was not stable and the surface coverage of the printed PbI_2 particles was incomplete (Figure 3c)).

At this point, the functionality of citric acid as the ligand was re-evaluated and also other approaches were considered. Several commercial dispersing agents were tested and they are listed in Table 2. The dispersing agent was mixed with the solvent system followed by adding the PbI_2-CA powder and mixing on the roller bench.

Table 2. The tested commercial dispersing agents (all purchased from BYK Additives & Instruments). The combination resulting into the most homogenous printed PbI_2 layer are shown in bold and underlined.

Disperbyk	Concentration (wt%)	Solvent
2012	5, 10, **20**, and 30	**3-7 EtOH:2BE**, H2O, EDGA, PGMEA, 2BEA
193	1, 3, and 6	3-7 EtOH:2BE, H2O, EDGA, PGMEA, 2BEA
190	**20** and 30	**3-7 EtOH:2BE**, H2O, EDGA, PGMEA, 2BEA

The PerTPV project has received funding from the European Union's Horizon 2020 research and innovation programme under grant agreement No 763977.

180	5 and 10	3-7 EtOH:2BE, H2O, EDGA, PGMEA, 2BEA

The effect of the dispersing agent additive was significant; the dispersion was stable for 3 weeks. Optical images and the corresponding SEM images of the printed PbI_2 layers are shown in Figure 4. The effect of the dispersing agent is seen as well-defined printed patterns and as a homogenous layer. As seen from the SEM images in Figure 4, the PbI_2 ink containing 20wt% DISPERBYK 2012® also results in decreased PbI_2 particle size and in a narrower size distribution (200-1000 nm without DISPERBYK® and 100-200 nm with DISPERBYK®).

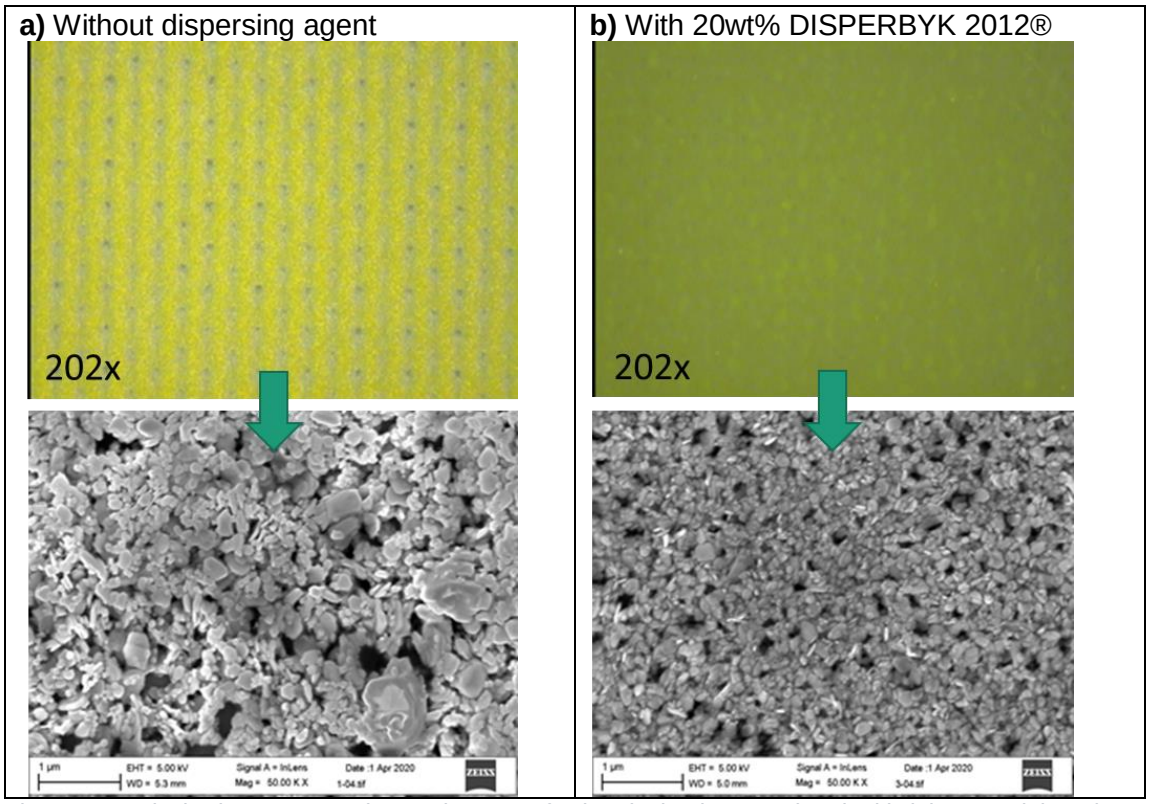

Figure 4. Optical microscope and SEM images of printed PbI_2 layers printed with inks containing a) no dispersing agent and b) with 20wt% dispersing agent.

Due to the limited solubility of CsI (a pre-cursor material in the conversion solution) in benign solvents, the dispersion fabrication method was further modified (Figure 5a)). In the final method, CsI was added into the PbI_2 dispersion enabling a broader testing of various concentrations and solvents of the conversion solutions. CsI was ground with citric acid and the powder was combined with the PbI_2 + citric acid powder after which the powders were added into the solvent system (mixture of ethanol and 2-butoxyethanol with a ratio of 3:7 v:v%). Finally, the grinding balls were added and the mixing was done on the roller bench for one week in an ambient environment (RT/humidity).

The PerTPV project has received funding from the European Union's Horizon 2020 research and innovation programme under grant agreement No 763977.

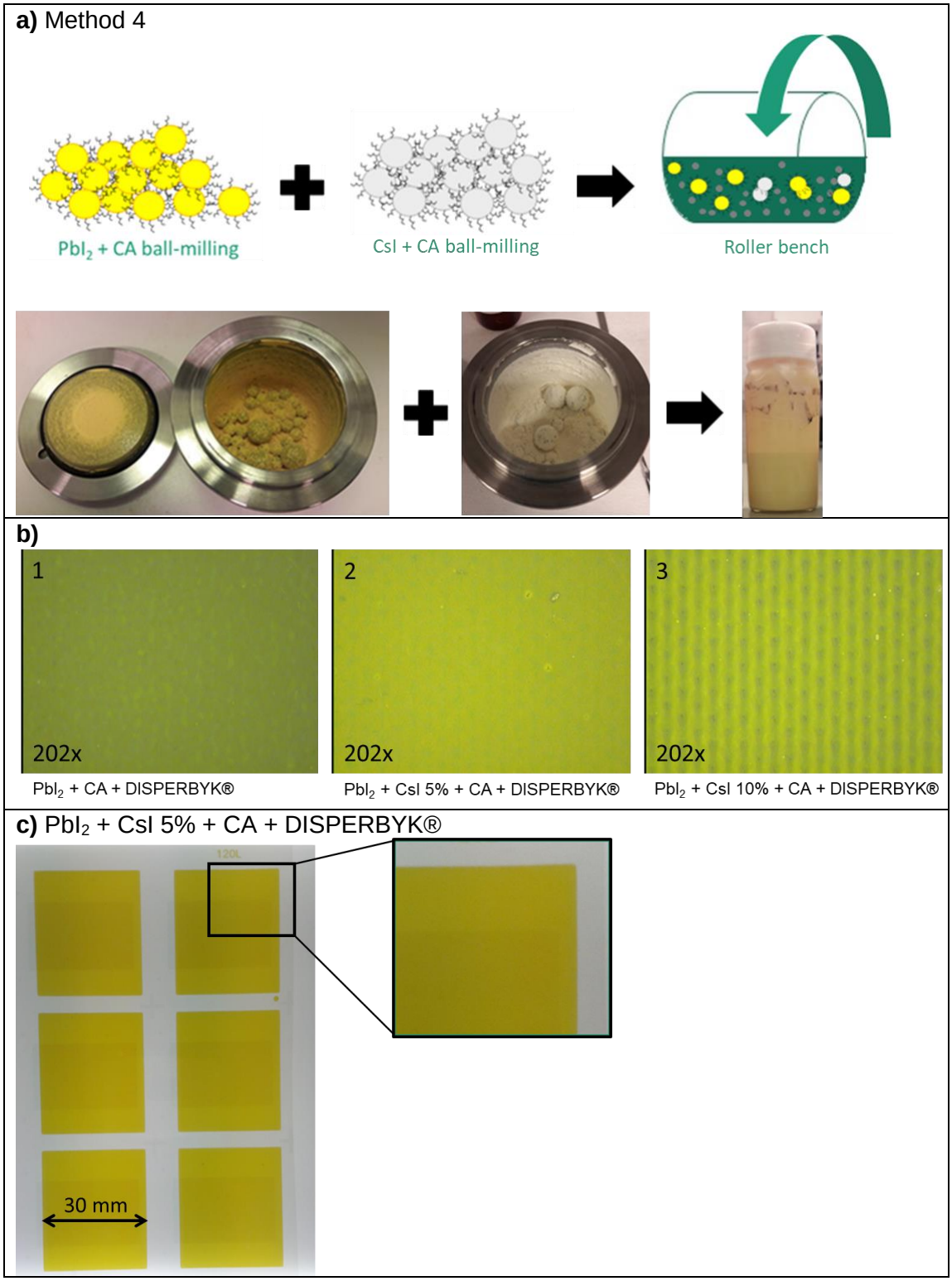

Figure 5. a) The final method utilised in the fabrication of PbI_2 + CsI dispersions. Also photographs of the ball milling equipment and the final ink dispersion are shown in a). b) Optical microscopic images (magnification 202x) of the corresponding printed PbI_2 and PbI_2 + CsI layers where the printing inks are made following the method shown in a). c) A photograph of a gravure printed PbI_2 + CsI layer into well-defined patterns.

As shown in Figure 5b) and c), this new type of ink led to an excellent layer quality: the substrate was fully covered with the ink, the layer was rather smooth, layer thickness

The PerTPV project has received funding from the European Union's Horizon 2020 research and innovation programme under grant agreement No 763977.

varied from 300 to 500 nm, and the particle size distribution was 100-500 nm including only a very few agglomerates.
Two CsI concentrations were tested (5 and 10 wt%) from which the 5 wt% resulted into more stable dispersion resulting to higher printing quality whereas the dispersion with 10 wt% was not stable leading to an incomplete surface coverage. This can be seen in the images in Figure 5b)

1.2.2 PbI_2 conversion to perovskite

After the preparation of the PbI_2 layer, the next step was to convert it into perovskite. The first experiments were conducted using a dip-coating method where the PbI_2-sample was immersed in the conversion solution where the reaction took place. Two conversion solutions were tested and they are listed in Table 3.

Table 3. Conversion solutions tested for dip- and bar-coating on top of printed PbI_2 layers.

Conversion solution	Ratio (mg/ml)
MAI:MACl in IPA	40 : 4
FAI:CsI:MACl in EtOH	62 : 5.2 : 1.4

The conversion proved to be challenging/sensitive due to the strong bonding of the ligands (citric acid and/or dispersing agent) with PbI_2 hindering the conversion.
After the first conversion experiments, the PbI_2 samples were washed with ethanol and/or water in order to remove the ligand from the PbI_2 particles opening spaces for the precursors and enabling the conversion. However, washing pre-treatment did not help because with the removal of the ligand, the PbI_2 layer was also de-attached from the substrate. Therefore, another deposition method for the conversion solution, bar-coating, was applied.
The same solutions from Table 3 were tested with bar-coating leading to improved conversion results in comparison with the dip-coating due to the decreased volume of the conversion solution deposited on top of the PbI_2-sample. On the other hand, the coating bar is in physical contact with the sample leading to some scratches and stripes and a partially damaged perovskite surface. The method was, however, seen as the most viable option for controlling the solution volume and the time it was in contact with the printed PbI_2 layers.
Also PbI_2 + CsI inks were converted into perovskite with bar coating. It was found that the presence of CsI improved the conversion and 5% concentration resulted in more complete perovskite conversion than 10%. The MACl in the conversion solution enhanced the film formation and the film appearance was shinier which typically refers to a homogenous and pinhole-free perovskite layer. Various solution concentrations were tested and they are listed in Table 4. An observation was made that the conversion is sensitive to the concentration of salts FAI and MACl in the solution. Based on XRD, UV-Vis and visual inspection data, FAI:MACl in isopropanol with 0.5M concentration led to the best perovskite layer quality.

Table 4. Conversion solutions tested for bar-coating on top of printed PbI_2 and PbI_2 + CsI layers.

Conversion solution	Ratio [mg/ml]	Concentrations [mol/l]
FAI:MACl in EtOH	9 : 1	0.4 – 1
FAI:MACl in EtOH	9.5 : 0.5	0.4 – 1
FAI:MAI in IPA	3 : 7	0.5 – 0.7
FAI:MACl in IPA:DMSO (99:1 v:v%)	9 : 1	0.25

a)	b)

The PerTPV project has received funding from the European Union's Horizon 2020 research and innovation programme under grant agreement No 763977.

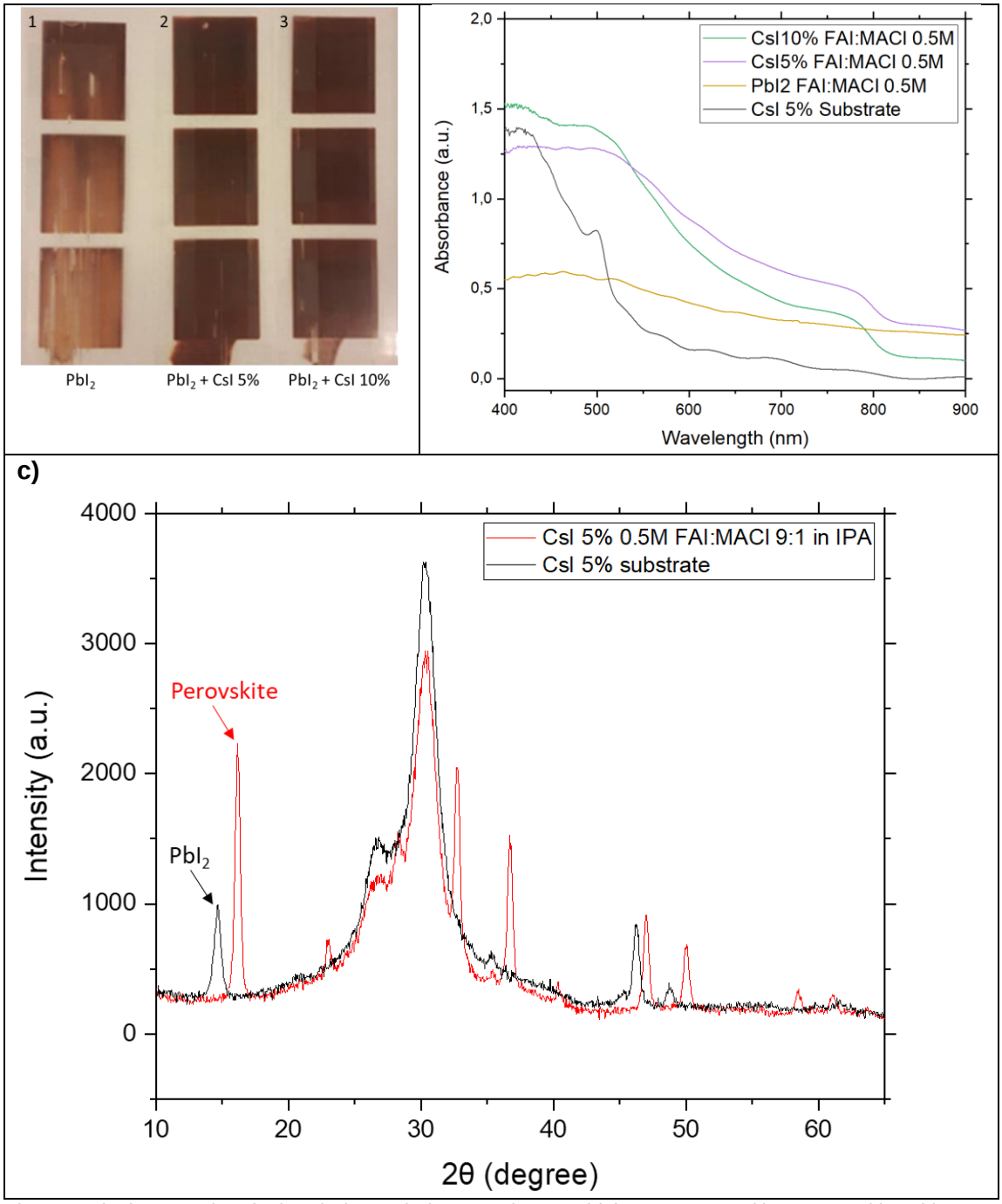

Figure 6. a) Photographs of printed PbI_2 and PbI_2 + CsI layers which are converted in to perovskite with 0.5M FAI:MACl 9:1 in IPA and b) the corresponding UV-Vis spectra. c) XRD spectra of the PbI_2 + 5% CsI layer (black spectrum) and the layer after conversion with 0.5M FAI:MACl 9:1 in IPA (red spectrum).

1.2.3 Summary and conclusions

To summarize, the first step, preparation of PbI_2 + CsI dispersion and printing the layer was achieved with great results: dispersion stability, patternability of the printing ink, surface coverage of the printed layer and layer thickness were all in the desired level. These results show that in the 2-step fabrication method, the use of toxic solvents (DMF, GBL) can be avoided using PbI_2 nanoparticle dispersions. The second step, conversion, proved to be challenging: the converted perovskite layers appeared hazy with some stripes due to the conversion solution and/or method. Optimizing the conversion solution and the deposition method of the conversion solution (bar coating, slot die coating etc.)

The PerTPV project has received funding from the European Union's Horizon 2020 research and innovation programme under grant agreement No 763977.

would still require more efforts. But due to the diminishing resources towards the end of the project, the developments could not be pursued further within this project. A suggestion for future work is that thermal processing of the PbI_2 + CsI film may be required, in order to drive off the organic ligands present from the dispersion agent. Due to the low thermal budget of the underlying flexible PET foils, rapid thermal annealing should be investigated, such as photonic curing.

2. Flexible single junction mini-modules

To achieve the ambitious target of 15 % PCE for the flexible mini-modules, three approaches were followed:

1. Deposition and patterning by printing at VTT
2. Deposition by spin-coating, patterning by laser at CSEM
3. Deposition by evaporation, patterning by shadow masking at UVEG.

At VTT, a n-i-p architecture with which 12.9 % PCE for 1 cm^2 area, flexible R2R-printed cells was utilized[3]. At CSEM, a p-i-n architecture with which PCE ~ 14 % at 1cm^2 when processed on glass was used. At UVEG, pin architecture with the expected PCE of 18 % at <1cm^2 area was used.

2.1 Gravure printed minimodules at VTT

As it became evident that the inks from benign solvents would not be able to deliver the 15 % power conversion efficiency target, a back-up solution was implemented. The inks and the cell architecture was based on a collaboration between VTT and Korea Research Institute of Chemical Technology (KRICT)[3]. The architecture was “nip” with the following materials: ITO as transparent cathode (R_s = 50 Ω/□), SnO_2 as ETL, $(FAPbI_3)_{0.95}(MAPbBr_3)_{0.05}$ as perovskite absorber, P3HT as HTL and gold (Au) as anode. For these printed solar modules, the SnO_2 nanoparticle ink and the $(FAPbI_3)_{0.95}(MAPbBr_3)_{0.05}$ perovskite inks were modified to achieve a proper viscosity and thus an adequate patterning of the printed layers. The module layout[4] is shown in the Figure 7a). In Figure 7b), the processing scheme for the modules is shown. Here, the R2R-patterned PET/ITO substrates were cut to sheets and the modules were finished with laboratory-scale printing equipment.

First, the ITO transparent electrode was R2R-patterned with a screen-printed etching paste. The SnO_2 aqueous nanoparticle ink was diluted to 2.5 wt-% with the final ratio of H_2O:IPA being 60:40 v:v-% and was printed on top of the O_2-plasma treated ITO with 120 lines/cm line density engraving. After annealing at 140°C for 10min and O_2-plasma treatment, the $(FAPbI_3)_{0.95}(MAPbBr_3)_{0.05}$ with 0.5 wt-% polyacrylic acid (PAA) dissolved in DMF:DMSO 8:1.5 v:v-% perovskite ink was gravure printed on top of the PET/ITO/SnO_2 samples. After printing, anti-solvent bathing with tert-Butanol:Ethyl acetate 1:1 v:v-% was used for 30 seconds followed by air blowing and thermal annealing at 140°C for 30min. P3HT (55 mg/ml in chlorobenzene:chloroform 4:1 v:v-% with Li-TFSI and tPB additives) was gravure printed on top of the perovskite layer and finally, the modules were capped with thermally evaporated 80 nm gold top electrodes.

[3] Kim, Y.Y. et al., Nat. Commun., 2020, 11, 5146, Roll-to-roll gravure-printed flexible perovskite solar cells using eco-friendly antisolvent bathing with wide processing window. https://doi.org/10.1038/s41467-020-18940-5

[4] The layouts were previously used in “pin” OPV-modules at VTT and thus, the “+” and the “-“ of the electrodes were the other way around than shown in Figure 7a) and b).

The PerTPV project has received funding from the European Union’s Horizon 2020 research and innovation programme under grant agreement No 763977.

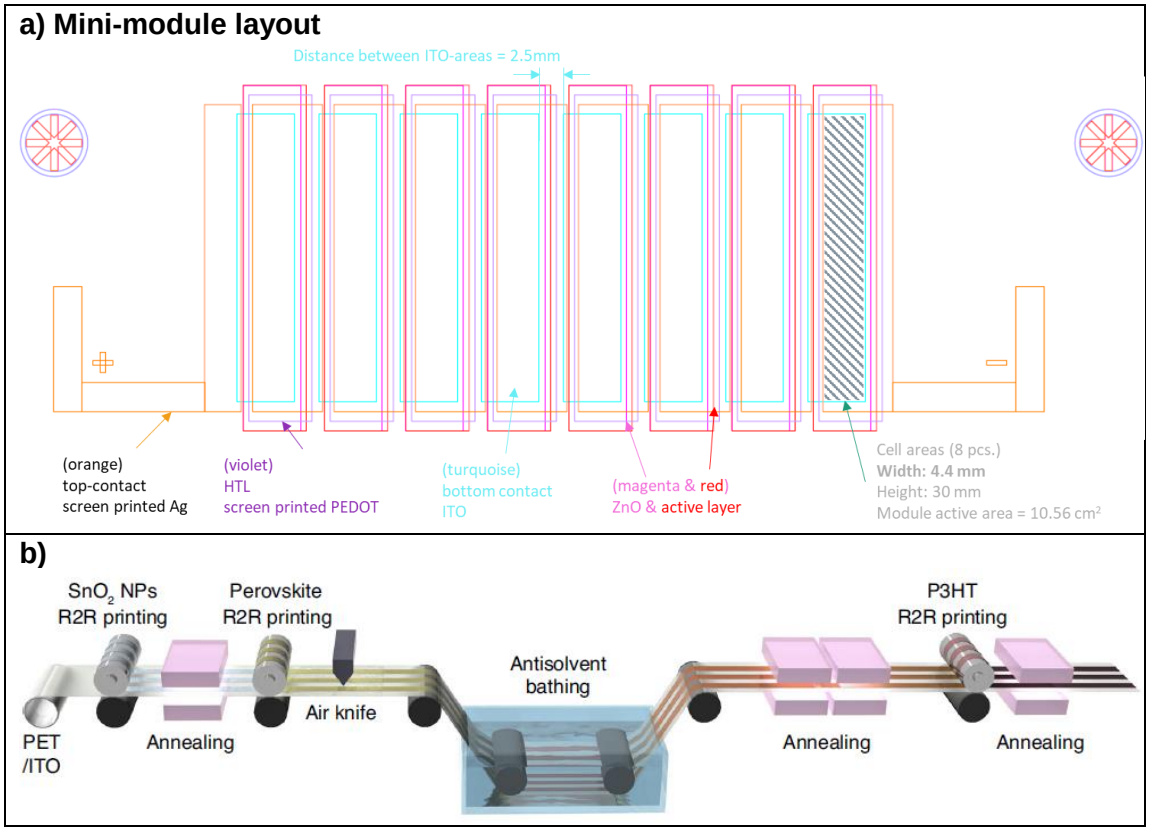

Figure 7. In a) the minimodule layout is shown (another layout with ITO width of 2.2 mm was also used). For the VTT mini-modules, SnO_2, $(FAPbI_3)_{0.95}(MAPbBr_3)_{0.05}$ and P3HT were all gravure printed with the "ZnO" layout. Additionally, instead of screen-printed Ag, an evaporated Au was used. In b), a schematic of the processing is shown (picture from Kim, Y.Y. et al., Nat. Commun., 2020, 11, 5146).

Two processing runs were made to achieve the printed modules and the solar parameters from 1st (module numbers 730-734) and 2nd (module numbers 741-750) runs are shown in Figure 8. The active area PCE of the champion module 731 was 6.22 % (with J_{SC} = 13.06 mA/cm^2, V_{OC} = 6.76 V and FF = 0.56) in reverse scan direction. Due to the hysteresis (mainly caused by the PAA viscosity modifier), PCE was decreased to 4.32 % in forward scan direction.

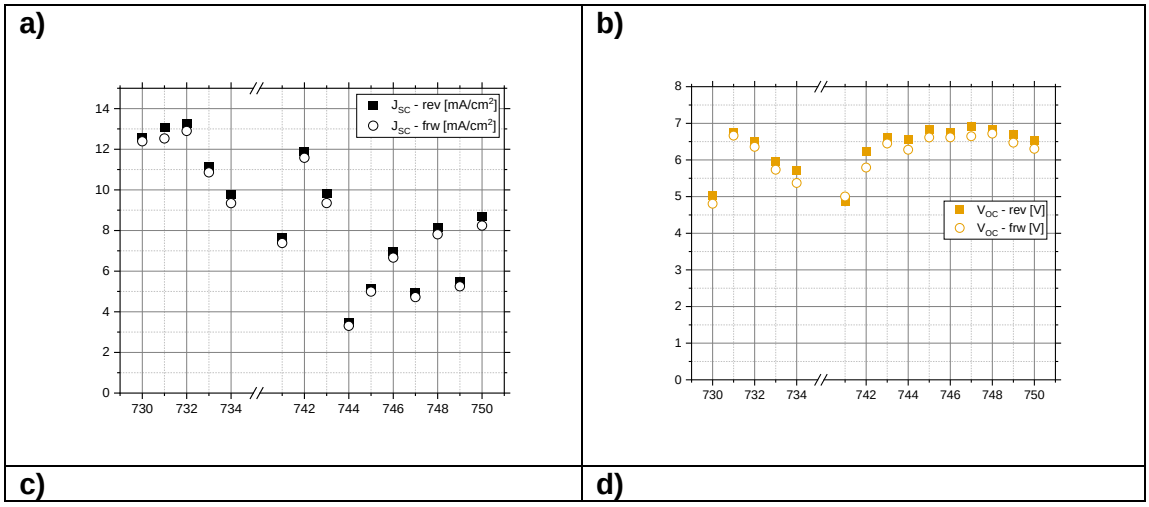

The PerTPV project has received funding from the European Union's Horizon 2020 research and innovation programme under grant agreement No 763977.

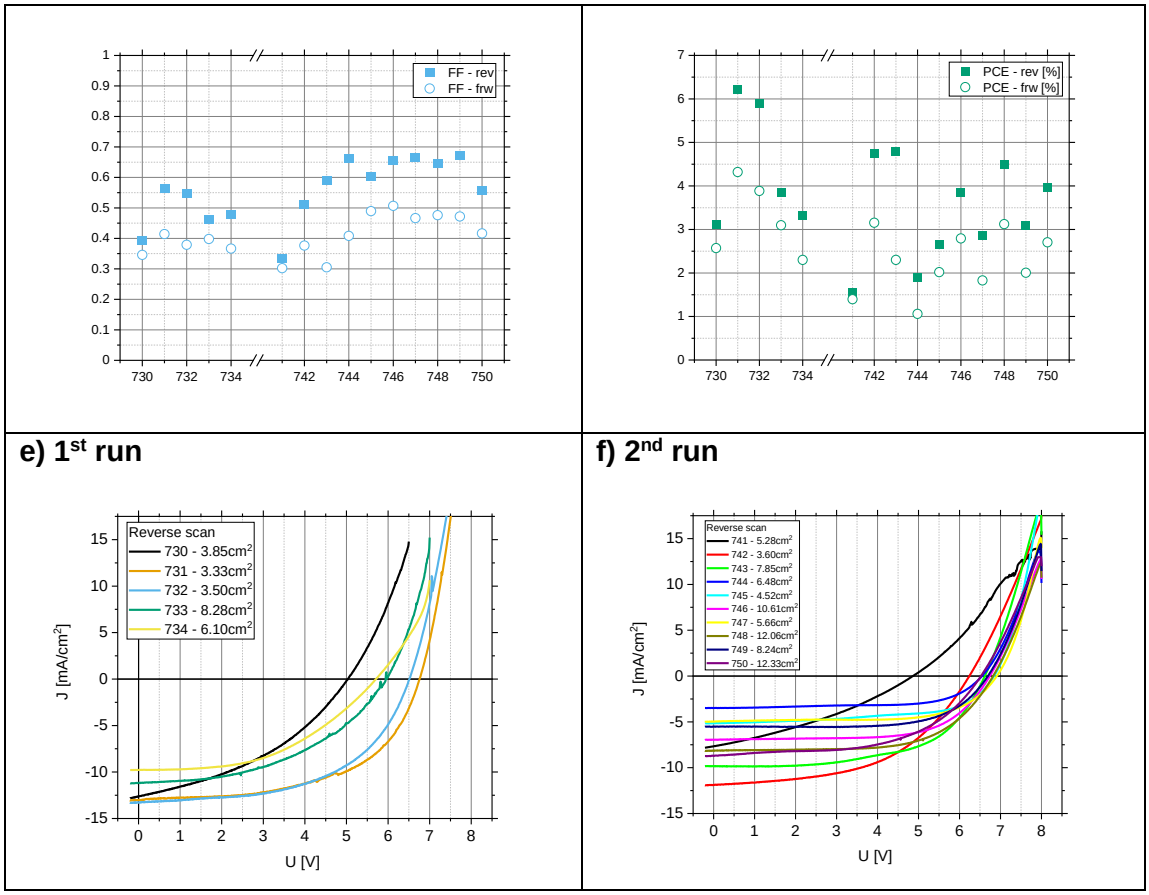

Figure 8. The solar parameters (a-d) and the corresponding JV-curves (e-f) of printed minimodules from processing runs 1 and 2. In the legends of e) and f), module number and the measured active areas are shown.

As seen in Figure 7, there is variation in measured results between modules processed in parallel indicating the sensitivity of the perovskite formation to the processing conditions *e.g.* the timing between deposition of the ink and anti-solvent bathing, intensity of the blow drying and temperature and humidity of the surroundings. It must be noted that in the R2R-environment, these variables can be controlled much more precisely than in laboratory scale where the processing is mainly done manually.

To summarize, a champion PCE of 6.22 % was achieved for modules with 8 cells monolithically connected in series and where the patterning of all layers, except the top electrode, was done by printing. It must be noted that a lot of time and effort was used for the development of perovskite inks from benign solvents and thus, there would be room for optimization and improvement in the results reported here. Though the targeted 15 % PCE was not achieved, these results show a very promising start on the way towards fully printed modules.

2.2 Spin-coated minimodules at CSEM

Minimodules at CSEM are made on 5x5 cm2 substrates by series connection of 5 segments through P1, P2 and P3 laser scribing. Figure 9 shows a schematics of the series interconnection. P1 is done on the TCO to define the segments, then all the cell layers except the top contact are deposited on full area and P2 is done to open the channels to the front TCO for the back contact deposition, which enables the series interconnection. Finally, after the back contact deposition on full area, P3 removes both back contact and perovskite and redefines the segments.

The PerTPV project has received funding from the European Union's Horizon 2020 research and innovation programme under grant agreement No 763977.

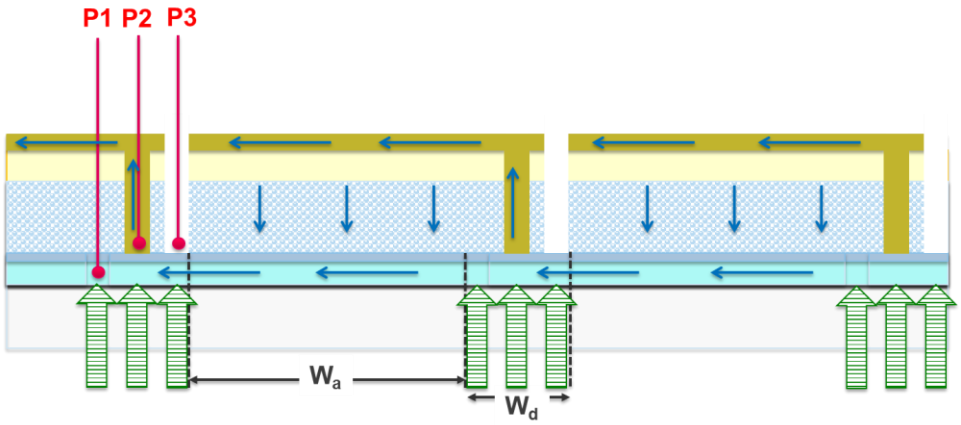

Figure 9. Schematics of a minimodule interconnection. W_a indicates the width of the active area and W_d the width of the dead area, i.e. the area between P1 and P3 that does not generate any power.

A green (515 nm) laser with a spot diameter of ~30μm and a pulse duration of 6 ps is used to scribe both TCO and perovskite. To scribe the TCO a higher energy is used as the TCO does not absorb green light as strongly as the perovskite. A few laser passes are used for P2 and P3, and also a conservatively large distance between P1 and P2, so that the width of the dead area is about 350 μm.

2.2.1 Preliminary tests on laser scribing on flexibles

A few laser scribing tests were done at CSEM on PET/ITO (R_s = 50 Ω/□) and PET/AZO/Ag/AZO (R_s = 10 Ω/□) substrates from VTT in order to assess whether the laser could scribe the TCO without melting the plastic substrates. Perfectly good isolation lines could be done in the PET/TCO substrates. The presence of a HTM on the TCO does not affect the scribing, therefore for practical reasons the P1 for the minimodules was done on substrates already coated with either PEDOT:PSS (Al4083):IPA 77:23 or NiO nanoparticles (2.5 wt% in butanols) by gravure printing at VTT.

2.2.2 Minimodules on VTT flexible substrates

To spin-coat the perovskite layer, the flexible substrates must be fixed to a glass support using an adhesive (Gel-Pak®). To keep the same alignment between P1, P2 and P3, the flexible substrates were fixed to the glass support before P1 and not removed until the last layer was processed. However the presence of the adhesive created some undesired light scattering and resulted in a non-continuous P1, as shown in Figure 10.

The PerTPV project has received funding from the European Union's Horizon 2020 research and innovation programme under grant agreement No 763977.

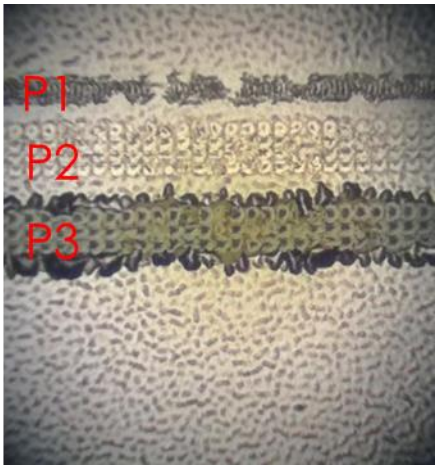

Figure 10. Microscope image of the laser scribing lines on a flexible substrate attached to glass support with GelPak adhesive. The P1 line does not appear continuous.

Minimodules were finished despite of the P1 issue. Substrates with NiO were exposed to 5 min UV ozone treatment to remove organics from the NiO nanoparticle layer. All the substrates were dried at 100°C under nitrogen for 30 min to remove residual moisture trapped in the plastic substrates. Then mixed-cation mixed-halide perovskite with composition $Cs_{0.17}FA_{0.83}Pb(I_{0.83}Br_{0.17})_3$ and bandgap 1.63 eV was spin-coated and annealed at 100°C for 30 min. The ETM consisting of 1 nm LiF and 20 nm C60 was thermally evaporated at 0.2 A/s at a pressure of 10^{-7} mbar, followed by 95 cycles of ALD SnO2 at 100°C (resulting in a 16 nm film). After P2, an opaque back contact consisting of ITO 70 nm /Ag 80 nm /ITO 70 nm was sputtered, followed by P3 laser scribing.

For IV testing, the minimodules should be removed from the rigid support, in order to gain in transparency. Figure 11 shows the back of a flexible minimodule before and after removal from the glass/adhesive. However, massive delamination of the back contact was apparent after removal. Therefore the minimodules were tested with illumination through the glass/adhesive. As expected for bad P1 lines, the minimodules were in short circuit.

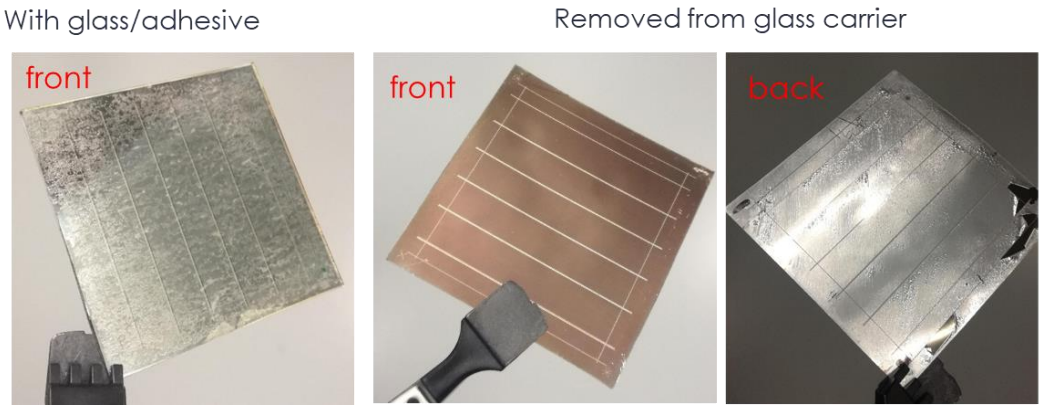

Figure 11. Photos of the flexible minimodule before and after removal from the glass carrier.

It is clear that series interconnection by laser scribing is much less suited to flexible substrates than for glass ones due to the laser alignment constraints and the importance

The PerTPV project has received funding from the European Union's Horizon 2020 research and innovation programme under grant agreement No 763977.

to keep the sample flat throughout the processing. Also, a bendable back contact has to be developed to be used with flexible substrates.

2.2.3 Small cells on VTT flexible substrates

In order to assess the maximum efficiency achievable on VTT flexible substrates using CSEM perovskite solution and processing methods, 1 cm^2 cells were fabricated with a stack ITO/NiO/SAM(Me4PACz)/$Cs_{0.17}FA_{0.83}Pb(I_{0.83}Br_{0.17})_3$/LiF/C60/BCP/Ag. NiO was annealed at 150°C for 30 min, SAM was spin-coated from a 1 mM solution in ethanol, the ETM stack LiF 1 nm /C60 20 nm/ BCP 5 nm was thermally evaporated, as well as the Ag back contact. For small cells P1 scribing line is also required but as there are no further scribing processes the alignment constraint is relieved so the flexible substrates do not have to be fixed to a rigid support. Moreover, spin-coating on a 2.5 x 2.5 cm2 substrate can be feasible without a rigid support.
The statistical analysis of the IV curves for the flexible cells and glass control cells is shown in Figure 12 and the best cell IV curve is shown in Figure 13.

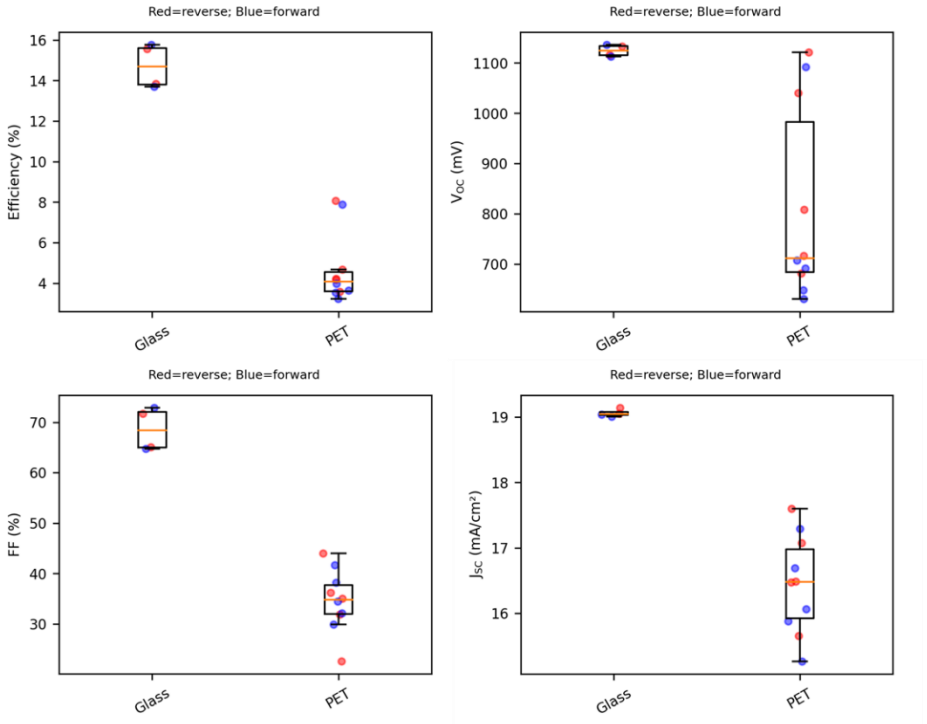

Figure 12. Statistical analysis of the IV curves obtained for cells on flexible and glass substrates.

The PerTPV project has received funding from the European Union's Horizon 2020 research and innovation programme under grant agreement No 763977.

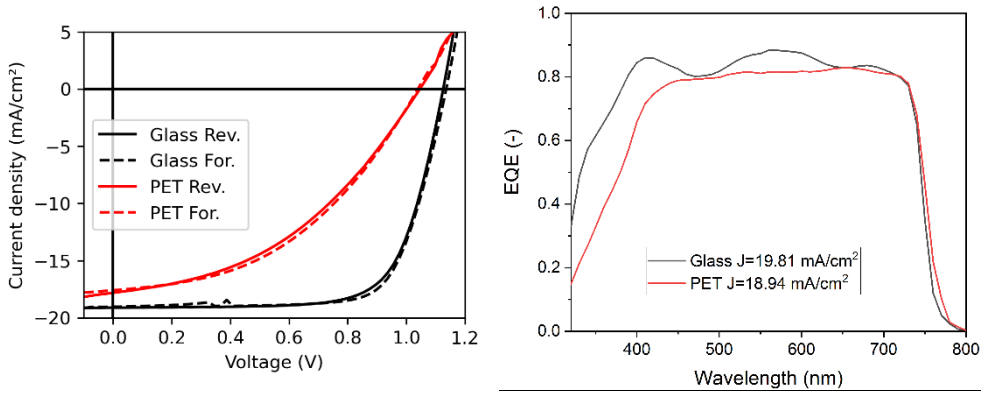

Figure 13. IV curves and EQE for the best rigid and flexible 1 cm² cells.

These results show that it is challenging to achieve good cells with the glass-optimized CSEM process on flexible substrates even for a 1 cm² cell size. The best cell, close to 8% efficiency, shows much worse FF and J_{sc} than the glass control cells.

2.3 Evaporated minimodules at UVEG

2.3.1 Evaporated minimodules on plastic foils with AZO/Ag/AZO transparent electrode

For these minimodules, ITO coated PET-substrates as developed by VTT and described in paragraph 2.1 (Figure 7a).
In view of the difficulties observed when attempting to laser pattern solar cells on flexible substrate (see paragraph 2.1.3.), we choose here to use a different approach to prepare different cells in series. As the semiconducting and absorber materials are deposited by vacuum sublimation methods, the area of deposition is controlled by the use of shadow masks. To demonstrate the proof of principle we did on purpose not attempt to search for the limits of resolution, but kept rather large spacings between each sub-cells. This off course leads to slightly non-optimal geometrical fill factors, but it reduces risks of shorts between the cells due to misalignment issues. In more industrial tools substrate handling is automated and there the risk of misalignment is easily avoided.
We developed substrate holders and evaporation masks that fit the dimensions of the foils supplied by VTT. Additionally, we had to adapt our test rig to fit these much larger substrates and align with the contact positions. The perovskite stack we used for this study was as follows (see also Fig. 14).

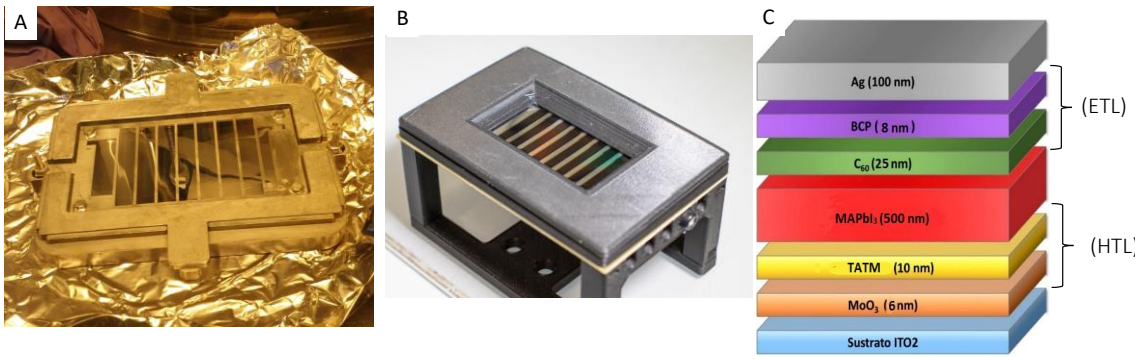

Figure 14. A. Substrate holder and shadow mask for the metal deposition. B. Dedicated test chuck for the large area foils. C. Layout of the perovskite solar cells stack.

The PerTPV project has received funding from the European Union's Horizon 2020 research and innovation programme under grant agreement No 763977.

In the first attempts we employed a thin layer of MoOx in between the transparent conducting electrode (ITO) and the hole transporting molecules (TaTm) to ensure an ohmic contact. However, this requires some mild annealing (100 °C for 10 minutes) which led to some damage of the foils. Therefore, we exchanged this MoOx layer for a layer of TaTm co-sublimed with the oxidizing molecule F6TCNNQ (with a thickness of 40 nm) which leads to a doped transport layer that also forms an ohmic contact and does not require annealing.

Our main concern with these large area substrates is the effect of dust particles in view of our academic research tools. The influence of dust becomes increasingly troublesome when increasing the active area of the devices. Again, like with the substrate handling also dust is not a real issue in large area industrial deposition tools. Hence, if in an academic lab, non-shorted devices can be prepared they would be improved in an industrial environment.

Our attempts, however, were successful in that it was possible to prepare a module in which all sub-cells are operating and contributing to the overall device performance. The J-V curve obtained while illuminating with an LED white light source set at 100 mW/cm2 intensity are shown in Figure 15.

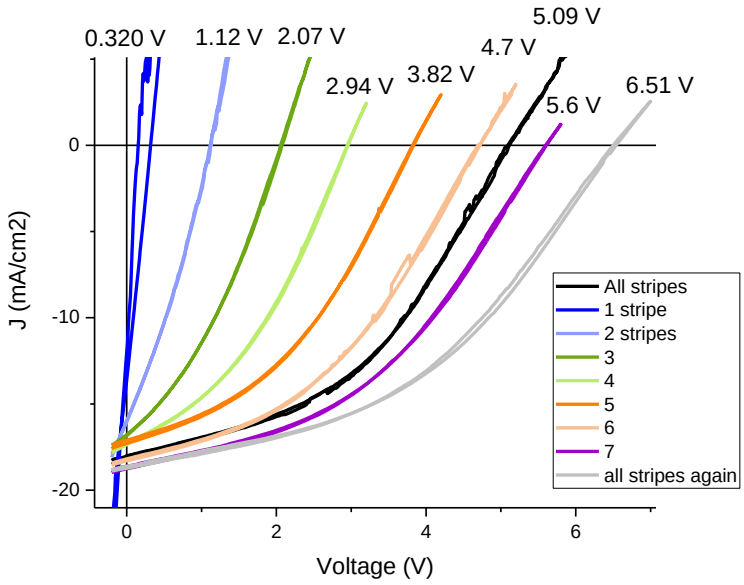

Figure 15. J-V curves of the flexible module according to the layout of Fig 14c but with doped TaTm as the first layer on the ITO. The cells were illuminated with a white LED light source set at 100 mW/cm2..

The total of 7 sub cells lead to a Voc of 6.5 volts, which implies that each cells has somewhat less than 1 volts. This is below what we normally obtain, and indicates some losses due to leakage (probably caused by the dust or imperfections on the foils). The current density is approximately 16.5 mA/cm2, which is determined by the least efficient cell. This is a rather decent value considering the large active area, and only 15 % below the value we obtain for small area cells on glass. The main issue, however, is the low FF with only 43 %. This we attribute to a too low conductivity of the used ITO transparent conducting substrate. We did attempt to employ a different TCO, based on PET-substrates with AZO/Ag/AZO from ROWO Coating GmbH. These were patterned at VTT and sent to UVEG for the cell processing. An iron nitrate ($Fe(NO_3)_3$) based screen printable etching gel developed at VTT was used for the patterning. Unfortunately, the

The PerTPV project has received funding from the European Union's Horizon 2020 research and innovation programme under grant agreement No 763977.

solar cells performance on these substrate were all shorted due to unidentified interactions with the TCO.

In Figure 16, a few photographs of the working large area flexible modules are shown that reached an efficiency of 5-6 %. Even though this is below the targeted values we feel it is a good result.

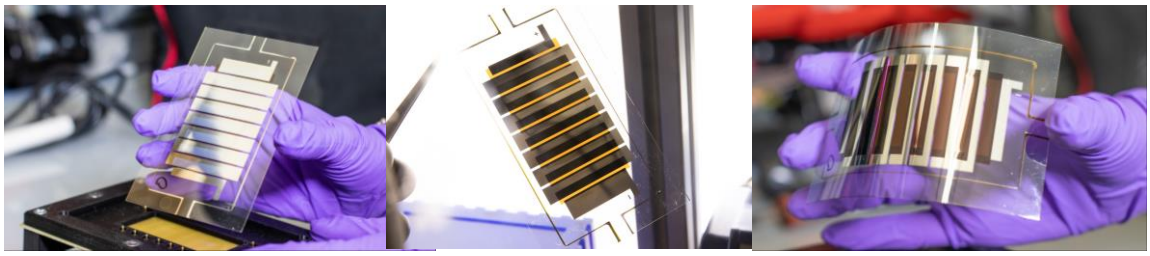

Figure 16. Photographs of the flexible large area modules prepared by patterning the foils (VTT) and depositing the solar cell stack using sublimation (UVEG).

2.3.2 Evaporated minimodules on metal (aluminium, copper) foils

As demonstrated in the previous sections, it is not trivial to divide large areas in subcells when the substrate is a polymer-based foil. Also, the alternative of depositing smaller solar cells separated using a shadow mask, did not lead to high efficiency modules due to the large losses due to the insufficiently conductive TCO.

A completely different approach is to attempt and make large area cells, not modules, hence without the series connection of sub-cells on a substrate, but rather use the complete substrate area to prepare one single cell. Due to the insufficient conductivity of the TCO's it is not possible to do this on a bottom transparent substrate unless grid lines are embedded in the substrate below the TCO. Such conductive grid lines are not transparent and hence to prevent too much loss in transmission, the grid lines must be narrow (< 0.1 mm). With such narrow lines their thickness needs to be at least in the micrometer size to reduce the series resistance of the transparent top electrode.

If however, the single junction cells employs a top transparent electrode, it is possible to place such thick grid lines on top of it. This method is also employed in commercial Si solar cells. And if the light enters the solar cell from the top, the bottom electrode on the substrate can be a non-transparent thick metal film that has a sufficiently high conductivity to extract all photogenerated carriers.
The main hurdle in this approach is the deposition of the TCO on top of the perovskite stack. Both CSEM and OXPV have developed a methodology based on sputtering and a protective interlayer. Recently, UVEG has developed a process based on pulsed laser deposition that enables the direct deposition of the TCO on the organic molecules employed as ETL in the perovskite stack.
We had developed this for small area cells on glass. The step from small area glass substrate to large area flexible substrate is too large. Therefore, we first evaluated if we can make a large area cell on glass. The structure is shown in Figure 17 and consist of a copper seed layer followed by a 70 nm Al layer. The remainder of the stack up to BCP is the same as in the previous section. The top electrode is a 140 nm ITO layer deposited using the PLD method developed by UVEG. To reduce the reflectance on the air/ITO interface we also added a 100 nm layer of LiF on top of the ITO. The right panel of Figure

The PerTPV project has received funding from the European Union's Horizon 2020 research and innovation programme under grant agreement No 763977.

17, contains an image of the small area pixels with and without the LiF anti-reflective layer (with a noticeable effect on the appearance).

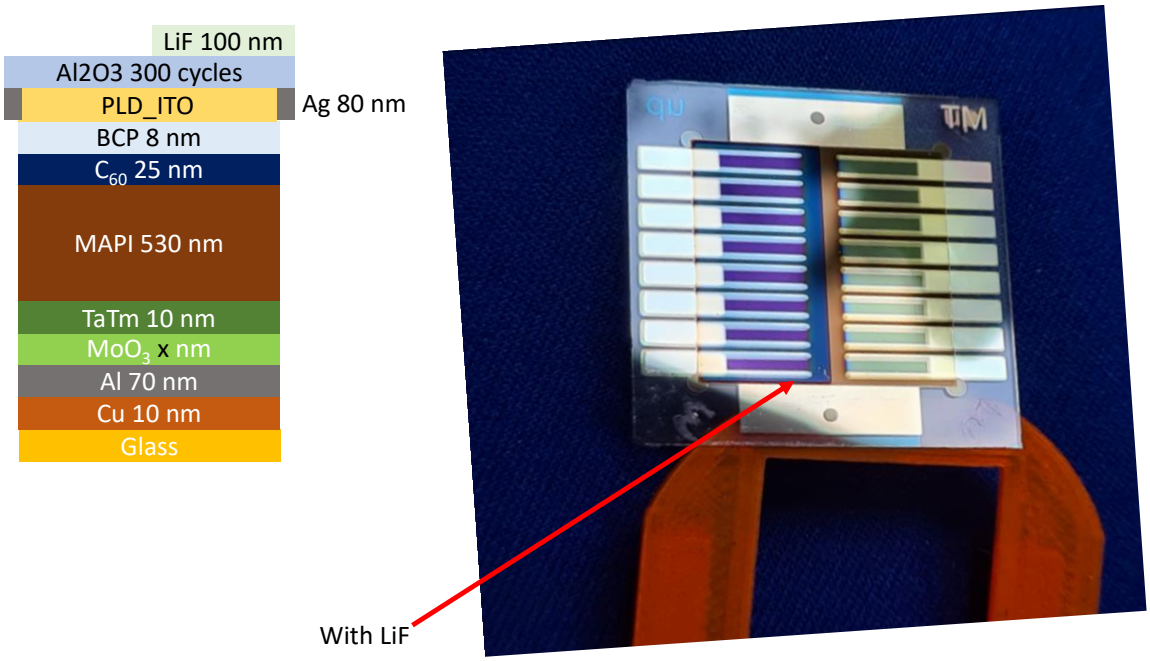

Figure 17. Stack of the bottom metal top ITO cells and right a photograph of such a small area rigid device.

Next we did the same process, without adjusting the layer thickness and attempted to prepare this on a 5 by 5 cm square glass substrate. For these larger areas it is important to add metal grid lines on top of the PLD ITO. Even though the large area cell are working the power conversion efficiency is slightly below that of the small area cells. Mainly due to loss of fill factor. In figure 18, J-V curve for the best cell is depicted as well as a few images of the 25 cm^2 cell.

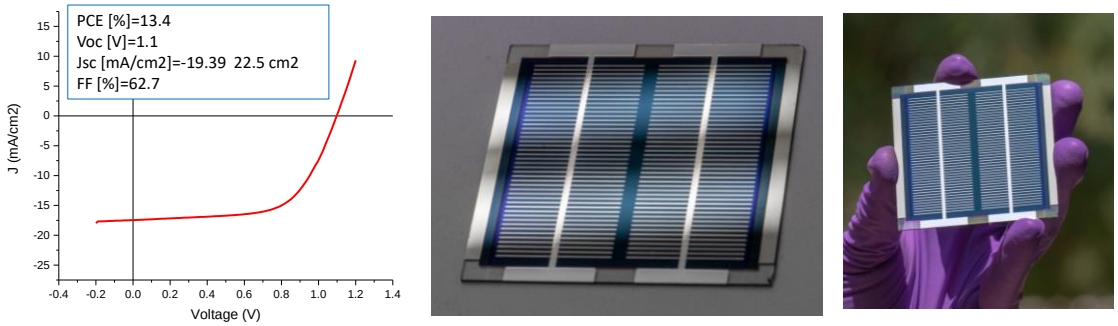

Figure 18. Stack of the bottom metal top ITO cells and right a photograph of such a small area rigid device.

After this successful demonstration of a large area single junction cell, we attempt to do the same on patterned cupper foils prepared by VTT (see Fig. 19.).

The PerTPV project has received funding from the European Union's Horizon 2020 research and innovation programme under grant agreement No 763977.

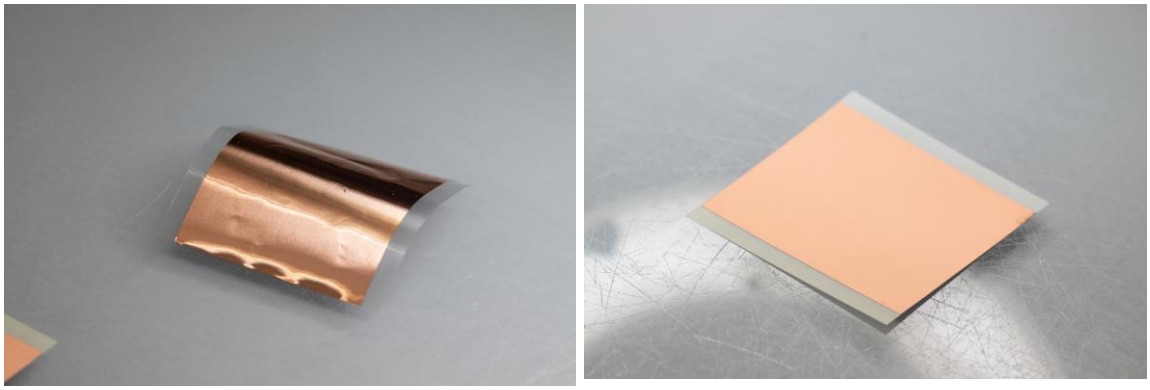

Figure 19. Two type of patterned Cupper on PET foils.

The handling of these foils is not as easy as large glass substrates, hence we had to laminate on top of a carrier substrate during processing. Unfortunately, most likely due to handling issues the final large area flexible cell was short-circuited. Some images of the finished devices are shown in Figure 20.

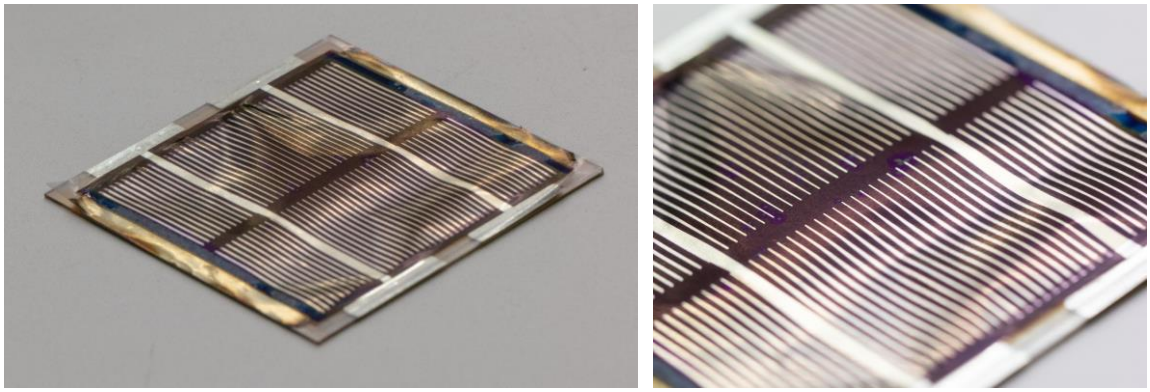

Figure 20. Photographs of the flexible large are foil attached to the carrier glass substrate.

Summary

The ultimate goal of PerTPV was to develop perovskite inks from benign solvents and to use them in the flexible single junction minimodules. For this purpose, both 1-step and 2-step conversions were investigated.

For the 1-step conversion, the Cyrene:H_2O solvent system resulted into very good printing inks with desired rheological properties. But the conversion of the printed layer to perovskite proved to be very challenging.

For the 2-step conversion, the first step, preparation of PbI_2 + CsI dispersion and printing the layer was achieved with great results: dispersion stability, patternability of the printing ink, surface coverage of the printed layer and layer thickness were all in the desired level. But the second step, conversion, proved to be challenging: the converted perovskite layers appeared hazy with some stripes due to the conversion solution and/or deposition method. Optimizing the conversion solution and the deposition method of the conversion solution (bar coating, slot die coating etc.) would have still required more efforts.

Thus, in the end, the printed and spin-coated modules were processed form the traditional DMF:DMSO solvent systems. All the spin-coted modules resulted in short circuits but with the printed modules, a champion PCE of 6.22 % was achieved for a module with 8 cells monolithically connected in series and where the patterning of all layers, except the top electrode, was done by printing.

The PerTPV project has received funding from the European Union's Horizon 2020 research and innovation programme under grant agreement No 763977.

It must be noted that a lot of time and effort was used for the development of perovskite inks from benign solvents and thus, there would be room for optimization and improvement in the results reported in this deliverable. Though the targeted 15 % PCE was not achieved, these results show a very promising start on the way towards fully printed modules.

The not foreseen efforts on sublimed single junction flexible modules and cells, was rather successful. We demonstrated working large area modules, albeit with still low efficiency of approximately 6 % which was due to the large series resistance of the transparent conducting oxide. At the end of the project, we showed the prospect of developing large area cells by depositing transparent top electrodes directly on the perovskite solar cells using pulsed laser deposition. The rigid substrates with an area of 25 cm^2 showed PCE of 13.4 % mainly limited by the FF. The translation to flexible substrates was hindered by handling issues. However, with the proper design of a carrier substrate and proper lamination this should be avoidable in the future.

The PerTPV project has received funding from the European Union's Horizon 2020 research and innovation programme under grant agreement No 763977.